(2)

Final Report • December 1992

FUNDAMENTAL ASPECTS OF METAL JOINING—THE STUDY OF STRONG INTERFACES

Anthony T. Paxton, Research Physicist
Mark van Schilfgaarde, Research Physicist
Physical Electronics Laboratory

SRI Project 3152

R&T Project Code: Met0032—01

Contract N00014-92-C-0006

Prepared for:

Office of Naval Research
Code ~~1311~~ 1131
800 North Quincy Street
Arlington, VA 22217-5000

Attn: Dr. George R. Yoder
Scientific Officer

Final Report • December 1992

FUNDAMENTAL ASPECTS OF METAL JOINING—THE STUDY OF STRONG INTERFACES

Anthony T. Paxton, Research Physicist
Mark van Schilfgaarde, Research Physicist
Physical Electronics Laboratory

SRI Project 3152

R&T Project Code: Met0032—01

Contract N00014-92-C-0006

Prepared for:

Office of Naval Research
Code 1311
800 North Quincy Street
Arlington, VA 22217-5000

Attn: Dr. George R. Yoder
Scientific Officer

Approved:

Ivor Brodie, Director
Physical Electronics Laboratory

Donald L. Nielson, Vice President
Computing and Engineering Sciences Division

SRI International 333 Ravenswood Avenue • Menlo Park, CA 94025-3493 • (415) 326-6200 • FAX (415) 326-5512 • Telex 334486

SUMMARY

Our aim for 1992 was to investigate whether modern quantum mechanical methods can be useful in the study of interfaces between dissimilar materials, and to complete at least a modest piece of work to demonstrate feasibility. This has been achieved.

We developed an *approximate* quantum mechanical approach to the problem of dissimilar transition-metal interfaces. Because of its approximate nature, we have devoted a large effort to testing the scheme against experiment and first-principles theory. Our expertise in local density functional theory has allowed us to draw upon our first-principles capability both in determining parameters for our model Hamiltonian, and in testing it.

We have studied in some detail a lattice-mismatched interface between pure Mo and Re metals (Section 2). Our conclusions concerning this system are that the shear strength of the interface is diminished from the theoretical strength by a factor of about twenty; the reduction is due to the presence of a misfit dislocation that glides in the interface during deformation. This factor is still some orders of magnitude smaller than the reduction of theoretical strength of perfect crystals by lattice dislocations. Therefore, while the strength of a mismatched interface is expected to be less than that of a lattice matched one (all other things being equal), the misfit dislocation is not expected to significantly weaken the bicrystal (Section 3).

In order that we can begin to study systems of arbitrary chemical compositon, such as aluminide alloys, nonmetal impurities in metal interfaces, and the metal-ceramic interface, we will need a general, first-principles, molecular-dynamics capability. Part of our proposal concerned our continuing development of such a scheme, and we report progress on this (Section 6).

In conclusion, in the short time available we believe useful results can emerge from quantum mechanical calculations that have some bearing upon engineering practice. Our work is sufficiently complete that we have some concrete results to report; at the same time there is much to continue in the same vein in the near future.

CONTENTS

FIGURES

TABLES

1. AIMS AND ACHIEVEMENTS

A large effort is under way to understand welded and diffusion-bonded joints between dissimilar materials. There is a number of outstanding questions concerning the weldability of traditional engineering materials. Also, newer materials are emerging and we want to learn how to bond them together. For example, modern ceramic materials allow the uses of very high engine temperatures and we need to know how to join these to underlying metal components. Hence, it is increasingly important to understand the metal-ceramic interface from a very fundamental point of view.[1] Certain refractory metals are again being developed for applications in nuclear engines and as energy convertors in the space program,[2] after having been set aside because they were thought less useful as engineering materials. An advantage of many of these metals is that they are *weldable*.[3]

The work undertaken for the present ONR contract is to study fundamental aspects of metal joining. The question is, whether recently developed quantum mechanical approaches to materials science can be useful in the context of the design of weldable materials. This is a high-risk program since so far no-one has attempted to use these new methods in the context of such complicated systems. However, the payoffs can be very great if this research will lead to our goal of first-principles criteria of weldability.

Certainly, the understanding of the strengths of dissimilar metal interfaces requires an investigation of the quantum mechanical nature of the bonding between atoms. A purely classical approach cannot arrive at a proper description, since the chemical bond is a quantum mechanical phenomenon. Therefore we require that our atomistic simulations of interface structure be quantum mechanically based, even if they cannot be completely "first-principles."

We intended that at the end of the first year (1992) we would have completed a feasibility study as well as arming ourselves with suitable results to make the first-year report describe a rather complete piece of research. *This we have accomplished.* We chose to pursue the following line of research:

1. Decide on a dissimilar metal interface to study.
2. Develop an approximate quantum mechanical description (Hamiltonian) for both metals and their alloys, which includes a prescription for interatomic forces.
3. Use molecular statics simulations to find the equilibrium, zero-temperature strength, and structure of the interface.
4. Evolve a plan of future work on this system.

These four items are discussed in the following four sections.

Our approach has been to use empirical quantum theory because current first-principles methods are too computer-intensive to be applicable to problems involving more than a few tens

of inequivalent atoms. Furthermore, the calculations of interatomic forces are still problematical. Both these difficulties can be removed using a new band-structure method that is currently under development. We briefly report progress on this in Section 6.

2. THE Mo/Re INTERFACE

As mentioned, there is renewed interest in refractory metals for use in high-temperature applications under conditions of hydrogen environments or neutron fluxes. For example, Mo, Re, and Mo-Re alloys are strong and ductile as well as weldable. We have chosen to investigate the strength of a Mo/Re interface.

This work takes us one step further in complexity from ideally lattice-matched interfaces, since the lattice constants, and indeed crystal structure, are different in these two metals. However, the c-axis in hcp Re is 4.46Å while the length of the face diagonal $a[1\bar{1}0]$ in bcc Mo is 4.45Å. Therefore an interface in which these two directions are parallel and in the interface plane will be lattice-matched at least in that direction. The Mo(110)/Re($10\bar{1}0$) interface contains these two directions, and if they are oriented parallel to each other, the orthogonal direction in the interface is parallel to the a-axes whose lengths are 3.15Å and 2.76Å in Mo and Re, respectively. The misfit along this direction is almost exactly in the ratio 7/8 so that the interface repeats itself every 7 Mo lattice constants and every 8 Re lattice constants, as illustrated in Figure 1.

In the general case of a lattice-mismatched interface, the mismatch occurs in two orthogonal directions and the expected equilibrium structure comprises a grid, or two-dimensional network, of misfit dislocations. This is a complicated case to treat; we simplify it by choosing an interface that is lattice-mismatched in only one direction. The expected structure is then a one-dimensional array of misfit dislocations similar to an array of edge dislocations in a low-angle-tilt grain boundary. We expect that this structure will provide much of the essential features of a lattice-mismatched interface except for the properties of dislocation intersections.

Our strategy is as follows. Taking the atomic arrangement shown in Figure 1(b)—the unrelaxed, or epitaxial interface—if we allow atoms to move according to the forces acting on them, how will the structure relax? Presumably the lattice mismatch will contrive to concentrate itself at the core of a misfit dislocation, which will be an edge dislocation lying in the interface plane with its line sense ξ parallel to the z-direction, normal to the plane of the paper in Figure 1(b). Having done this relaxation, or atomistic simulation we will initially ask two questions:

1. What is the width of the core?
2. What is the size of the Peierls barrier for dislocation motion? In effect, what is the shear strength of this ideal interface? Later, we can then ask such questions such as What is the effect of interdiffusion on the strength? and What is the effect of the point defect dislocation interaction?

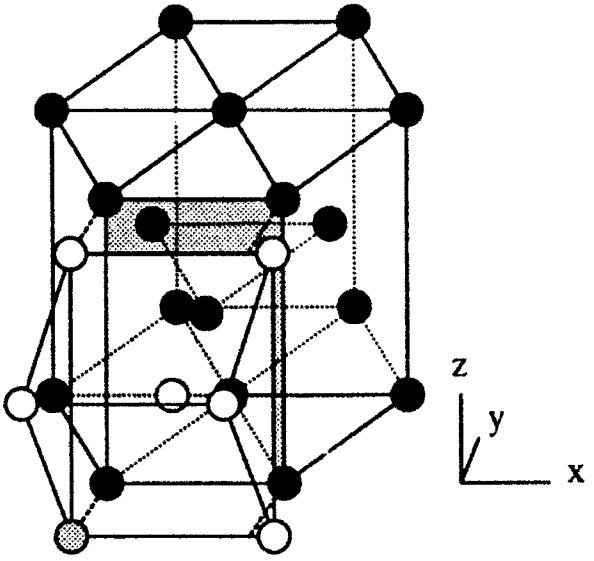

(a) Juxtapostion of the Re hcp and Mo bcc lattices. Planes parallel to the interface are shown shaded. The *z*-direction is parallel to $[1\bar{1}0]_{Mo}$ and $[0001]_{Re}$. In this direction, the structure repeats itself every repeat of the hcp *c*-axis, which is equal in length to $\sqrt{2}\, a_{Mo}$. The *x*-direction also lies in the interface and is parallel to the *a*-axes of Mo and Re which differ in length in the ratio 8/7; the interface is therefore mismatched in this direction but repeats every 7 Mo and every 8 Re lattice spacings *a*. The *y*-direction is normal to the interface and parallel to $[110]_{Mo}$ and $[10\bar{1}0]_{Re}$. The distance *h* between the two crystals is shown as a broken line. The total energy will be minimized with respect to *h*.

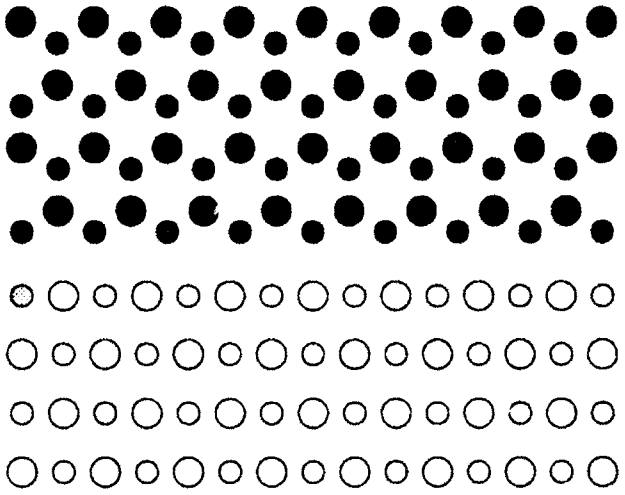

(b) A projection of the Mo/Re interface down the *z*-axis of Figure 1(a). Only two planes of atoms need be shown in this direction as the structure then repeats itself. These two planes are shown as large and small atoms. The *x*-axis points to the right and the figure shows 7 Mo and 8 Re lattice spacings in this direction after which the structure repeats itself. The *y*-axis points upward. Note disregistry in the interplanar spacing across the interface. The same Mo atom in both figures is slightly shaded to emphasize the relation between the two perspectives.

Figure 1. Mo/Re interface.

3. TOTAL ENERGY AND INTERATOMIC FORCES

3.1 THE TIGHT-BINDING FORMALISM IN RELATION TO DENSITY FUNCTIONAL THEORY

As mentioned in Section 2, we will require a means to calculate the forces acting upon Mo and Re atoms in a solid-state assembly of these atoms. A traditional approach would be to develop a pair-potential or Finnis-Sinclair[4] model to describe the interatomic interactions. This is not always possible, particularly as we shall see below in the Mo-Re system, and is never reliable. We take the view that interatomic interactions are quantum mechanical in nature and can only be correctly calculated by solving a Schrödinger equation for the electrons responsible for bonding in the solid state. Our usual approach is, in fact, a first-principles approach: we use density functional theory to study the properties of transition metals and alloys.[5,6] In the present situation, however, a completely first-principles approach is out of the question. First the *ab initio* density functional theory is too computer intensive for such complicated problems, and second, there are difficulties involved in calculating interatomic forces in transition metals.

We have therefore chosen to do our calculations within the tight-binding approximation to the electronic structure problem. Our approach is similar to that of Sutton *et al.*[7] The way the tight-binding method works is this: We know which electrons are most responsible for bonding in the central transition metals (namely the *d*-electrons), and we know the basic form that the Hamiltonian must take. So, instead of computing the Hamiltonian self-consistently, which is very time consuming, we *parameterize* its matrix elements, after which we solve the Schrödinger equation just as in the first-principles approach to obtain eigenvalues ε_i and eigenvectors c_i.

In density functional theory, the (negative) cohesive energy is

$$E_B[\rho] = \sum_{i,occ} \varepsilon_i - \frac{1}{2}\int dr\, \phi_{es}\rho(r) - \int dr \mu_{xc}\rho(r) + E_{xc} + E_{ii} - E_{atoms} \quad . \tag{1}$$

The sum is over occupied eigenvalues; ρ is the electron density; ϕ_{es} is the classical electrostatic potential of the density:*

$$\nabla^2\phi_{es} = -8\pi\,(\rho - \rho^+) \quad , \tag{2}$$

where ρ^+ is the density of positive charges (nuclei); E_{xc} is the exchange and correlation energy; μ_{xc} is the exchange and correlation potential:

$$\mu_{xc} = \frac{\delta E_{xc}[\rho]}{\delta\rho} \quad .$$

---

* We will use attomic Rydberg units (a.u.) throughout: $\hbar^2/2m = 1$ and $e^2 = 2$. 1 Ry = 13.6 eV and the unit of length, 1 bohr = 0.529Å.

E_{ii} is the electrostatic pair repulsion between the ion cores, and E_{atoms} is the total energy of the free atoms *in vacuo*.

In density functional theory, ε and **c** are eigenvalues and eigenvectors of the *effective, single-particle* Hamiltonian

$$\hat{H} = \nabla^2 + \upsilon_{eff}(r)$$

(in atomic units). The Schrödinger equation,

$$\hat{H}\,\mathbf{c_i} = \mathbf{e_i}\,\mathbf{c_i}$$

must be solved self-consistently with the Poisson equation, Eq. (2), since the effective potential

$$\upsilon_{eff} = \phi_{es} + \mu_{xc}$$

depends on the charge density through Eq. (2).

In tight-binding theory the cohesive energy usually takes the general form[7,8]

$$\tilde{E}_B = \sum_{i,occ} \tilde{\varepsilon}_i + \tilde{E}_{rep} + C \quad , \tag{3}$$

where $\tilde{\varepsilon}$ are the eigenvalues of the parameterized tight-binding Hamiltonian, and $\tilde{E}_{rep} + C$ is supposed to represent the rest of the terms in Eq. (1) with the constant C fixing the zero of energy with respect to the free atoms. $\tilde{E}_{rep}$ has the form of a pair potential. Sutton *et al.*[7] were able to justify this form rigorously using the Harris approximation to the self-consistency procedure. In their approach, the repulsive energy represents the changes in electrostatic and exchange-correlation energies in going from free atoms to the solid state and could be shown (to a very good approximation) to be a pairwise repulsive energy.

In problems of dissimilar interfaces, it has been argued (see M.W. Finnis[1]) that a completely non-self-consistent approach is inappropriate. We therefore use a self-consistent, tight-binding scheme.[9] We want the Hamiltonian to be able to respond to changes in the potential, at least in its diagonal matrix elements. This is done in the following way: After solving the Schrödinger equation for the tight-binding Hamiltonian, there will be accumulations of charge Δq_k on each atom k. These accumulations will give rise to an approximate electrostatic potential (again in atomic units, $e^2 = 2$)

$$\tilde{\phi}_j = \sum_{k(\neq j)} \frac{2}{|r_k - r_j|} \Delta q_k + 2U\Delta q_j$$

on atom j. This is a sum of two terms:[10] the first is the interatomic, Madelung potential assuming the charge on each atom behaves as a point charge; the second is the intraatomic potential, which has the opposite sign and represents the energy penalty of heaping charge onto an atom. The two terms may both be large, but mostly they tend to cancel each other.[10,11] The parameter U is sometimes called the *Hubbard U*. $\tilde{\phi}_j$ is then the electrostatic potential at atomic site j that is seen by an electron described by the tight-binding Hamiltonian. We then adjust the diagonal elements of the Hamiltonian by adding the $\tilde{\phi}_j$ at each site and solve the Schrödinger equation again to obtain a new electrostatic potential. This procedure continues until self-consistency is reached. In this way, the off-diagonal matrix elements remain fixed by their values determined

by the parameterization, while the diagonal matrix elements are determined self-consistently. At self-consistency, the electrostatic energy (which must be included in the tight-binding energy) is

$$\tilde{E}_{es} = \frac{1}{2}\sum_j \tilde{\phi}\Delta q_j \quad .$$

Because of the large cancellation between terms, this energy is usually so small as to be negligible, as pointed out by Harrison.[10]

Let us now write down the cohesive energy in tight-binding for a transition metal in which we include only *d*-electrons in the Hamiltonian. The off-diagonal matrix elements are transfer integrals between *d*-orbitals on different sites and are determined by parameterization, as discussed below. The diagonal matrix elements are determined self-consistently. We also will choose a fixed number of *d*-electrons for each transition metal: The number is N_d^k for the atom type at the position labeled k. Electrons will transfer between sites self-consistently unless a charge neutrality condition is imposed,[7] which amounts to setting $U = \infty$; in reality, U is closer to about 10 eV. The input number of *d*-electrons will be used in setting the constant C in Eq. (3); this is only constant, however, in non-selfconsistent tight-binding where the diagonal elements of the tight-binding Hamiltonian $\tilde{H}_{kk}$ are constants.[7] The cohesive energy is

$$\tilde{E}_B = \sum_{i,occ} \tilde{\varepsilon}_i - \sum_k N_d^k \tilde{H}_{kk} + \tilde{E}_{rep} + \tilde{E}_{es} \quad . \tag{4}$$

Except for the last term, this is the same expression given by Paxton and Sutton.[12]

It is not difficult to differentiate this expression to obtain interatomic forces. Chadi[13] and Kohyama *et al.*[14] give details. In the present work, we do make the approximation that only the first term and $\tilde{E}_{rep}$ contribute to the force on an atom.

3.2 PARAMETERIZATION OF THE HAMILTONIAN

We need to find parameters for the Hamiltonian matrix elements and the pair potentials that make up $\tilde{E}_{rep}$. We also need values for the Hubbard U parameter. It is in this sense that the tight-binding method is empirical rather than first-principles and, for this reason, we will have to test the parameters we use to ensure that they give sensible results for the known properties of Mo and Re. We can then apply the parameterized Hamiltonian to the problem of the strength and structure of interfaces with confidence.

The tight-binding theory of transition metals is well developed and goes back some 20 years.[15] In fact the method has been practically applied with great success long before Sutton *et al.*[7] and Foulkes and Haydock[16] made the connection between tight-binding and density functional theories. There are two uncertainties in the method. First is the assumption that the Hamiltonian can be parameterized and that the remaining energy can be cast in pair-wise form. Second is the need to find functional forms and parameters for the Hamiltonian matrix elements and the pair potential. Specifically, these forms and parameters need to depend only on the distance between the two atoms in question and the types of atoms involved. Implicit in this is the further assumption that the Hamiltonian is "two-center"; that is, it has no terms involving three atoms simultaneously. This is closely connected with a final assumption, namely that the Hamiltonian appears in an orthogonal representation. Both nonorthogonality and three-center

terms are known to vanish to first order in the band theory of transition metals. Given that the first assumption is rigorously defensible from within density functional theory, we are left with the selection of parameters that will yield an adequate description of the transition metals in ques-tion. Nevertheless, because this is an empirical method, we need to make exhaustive tests of the model to show that it is suitable for use in atomistic simulation.

Two functional forms are popular for the Hamiltonian matrix elements and the pair potential. In the canonical model, the distance dependence is the inverse fifth power for the matrix elements and some larger power (around 10) for the pair potential. While this is the model that derives naturally from band theory,[17] we have found in the present work that it fails to reproduce structural energy ordering as described below. Instead, we have found the model of Spanjaard and Desjonquères[18] to be the most robust and reliable. In this model, the two center matrix element of the Hamiltonian connecting two atoms separated by a distance r takes the form $h(r) = -fe^{-qr}$ and a pair potential of the form $\varphi(r) = be^{-pr}$ is used. Spanjaard and Desjonqueres find $p/q = 2.95$ by comparison with the Rose equation of state and tabulate values of p and q for all the transition metals. We do not argue that there is any physical basis for their choice of p and q, but we do find that these are sensible parameters. The outcome of any calculation must anyway be insensitive to details of the parameter choice, and this is indeed the case. Given p and q for Mo and Re, we have only two free parameters for each metal, namely the prefactors f and b. We will adjust b to obtain the correct lattice constant (atomic volume) and f will be chosen to obtain the same width of the d-band as found in a self-consistent band calculation. Finally, the ratio of the $dd\sigma$:$dd\pi$:$dd\delta$ is given the usual canonical form, 6:-4:1.

We should point out that our model includes only d-electrons in the Hamiltonian. The effect of the s-electrons is to provide a positive pressure, which is included in the repulsive pairwise term. The number of d-electrons N_d is therefore a parameter, not neccessarily the number of d electrons in the free atom. The cohesive energy in Eq. (4) is therefore not determined strictly with respect to free atoms but to some vacuum reference state in which the number of d-electrons is N_d. The most sensible choice of N_d should come from exact band calculations, in which case, we find 4.39 d-electrons in Mo and 5.12 in Re. The difference is less than one because the 5d series have more s electrons, in general, than the 4d (Figure 2). What is startling is that in Mo the bcc structure is strongly favored, while the bcc structure is very unfavorable in Re. Figure 2 shows hcp-fcc and bcc-fcc energy differences calculated using band theory. It is well known that what determines the stability of transition metals is simply the number of d electrons. However, the rapid rise in the bcc-fcc energy difference with a change in N_d of less than one cannot be reproduced in a simple tight-binding model without sd-hybridization.[20] We will return to some of these points later, but for now we mention that we have tried adjusting N_d and found that the best value for Mo is the band theory value of 4.39; however, if we choose 5.12 in Re, then the bcc structure is stabilized, so that to guarantee the correct ordering of crystal structures we have to set $N_d^{Re} = 6$.

Finally, we need to determine the Hubbard U parameter, and for this also we turn to density functional theory. We use the LMTO-ASA method in the following way. First, we make a self-consistent calculation of the atomic sphere charge density and logarithmic derivatives in Mo and Re at equlibrium volume. Keeping the boundary conditions fixed, we add a small charge dq_d into the d-electron channel and recompute the total energy of the atomic sphere

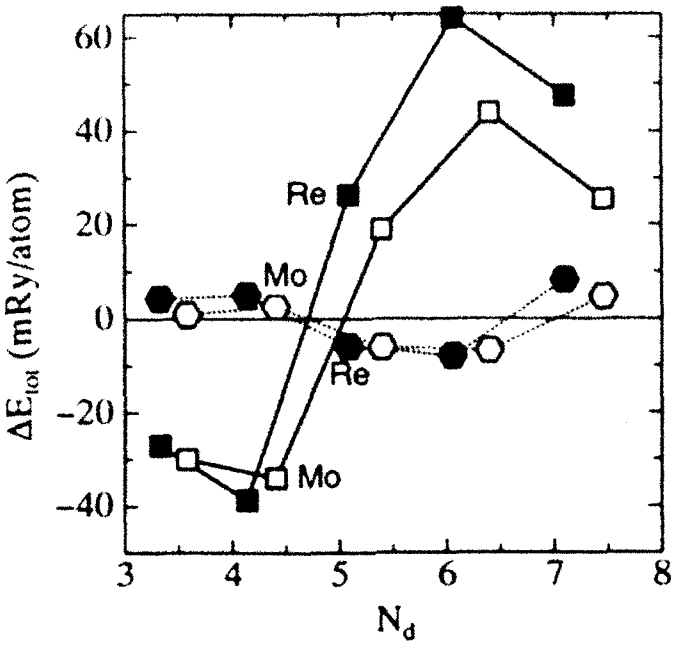

Figure 2. Energy differences between the bcc and fcc lattices (squares) and hcp and fcc lattices (hexagons) in the 4*d* (open symbols) and 5*d* (closed symbols) central transition metals (groups 5–9).[19] Both the energies and *d*-electron numbers are determined from band theory. Note the rapid destabilization of the bcc phase over a very small change in N_d. This effect cannot be reproduced in a simple *d*-band tight-binding model.[20]

We then use

$$U_d = \left.\frac{d^2 E_{tot}}{dq_d^2}\right|_{dq=0}$$

to determine the Coulomb integral U for the d electrons. This is illustrated in Figure 3.

The parameters for Mo and Re thus determined are displayed in Table 1. (Those for Re have been slightly adjusted to make the conditions $c_{Re} = \sqrt{2}a_{Mo}$ and $a_{Mo}/a_{Re} = 8/7$ exact.) It only remains to specify the interactions between dissimilar atoms. For these, we use the geometric means of the pure atom interactions, which is the correct combination according to band theory.

Table 1

PARAMETERS FOR THE TIGHT-BINDING MODEL FOR Mo AND Re
(All numbers are in atomic units)

	p	*q*	*f*	*b*	N_d	*U*
Mo	1.9513	0.6621	0.4679	1408.8	4.39	0.854
Re	2.0316	0.6687	0.5900	1893.9	6.00	0.872

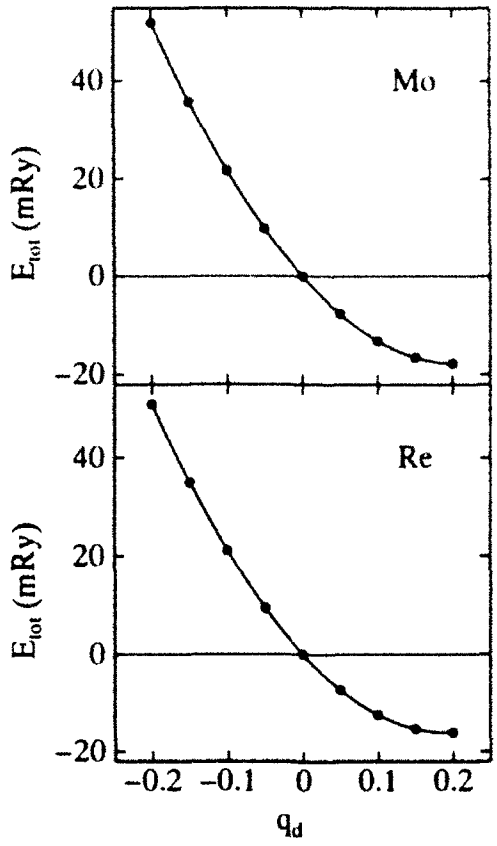

Figure 3. Total energy in the local density approximation for Mo and Re as a function of a small excess *d*-electron charge. The curvature of these curves for the neutral solid is the Hubbard *U* parameter.

3.3 TESTS OF THE HAMILTONIAN

As mentioned, we want to test the tight-binding model extensively before applying it to the Mo/Re interface. The tests fall into two categories: tests of the cohesive and elastic properties of the equilibrium structure, and tests of structural stability in which the atomic coordination is radically different from the equilibrium structure. We will also test the finite strain-deformation behavior. These are described in the following three subsections.

3.3.1 Equilibrium and Cohesive Properties

We do not expect to be able to reproduce the experimental cohesive energy in our model. This is contrary to previous claims[18,21] that have been made. Indeed, the cohesive energy does come out in quite good agreement with experiment if one ignores the spin polarization of the free atom. However, this spin polarization is very large (about 0.2 Ry) in the central transition metals and cannot be neglected. If it is included, then we find a cohesive energy of about 2/3 the experimental value. The remaining 1/3 is due to *sd* hybridization, which is not in the model (see Figure 4). Obviously, one could then ask, why not include the *s*-band? And the answer is twofold.

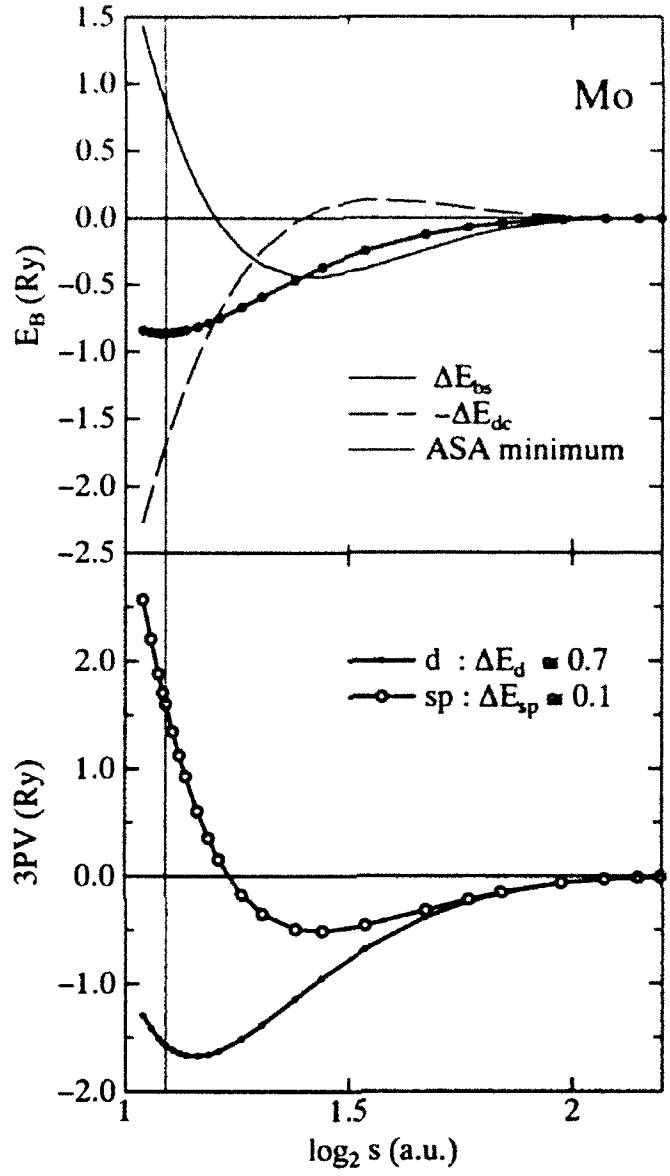

Figure 4. Band theory calculations of the contributions to the cohesive energy (top panel) and pressure (lower panel) as non-spin-polarized Mo atoms are brought from infinity in the vacuum together to form the bcc crystal. The equilibrium volume is indicated by a vertical dotted line; and there we see that the cohesion is a balance of a band contribution ΔE_{bs}, which is the first term in Eq. (1) and renormalization contribution ΔE_{dc} which represents the other terms in Eq. (1). In the lower panel, we see clearly that the *d*-electron contribution to the pressure is negative (attractive) and the contribution from the free-electron-like *sp*-electrons is positive. As noted in the text, this latter effect cannot be reproduced in a simple tight-binding band theory and is relegated to the repulsive pair-potential. The atomic volume is represented as the logarithm of the Wigner–Seitz radius s in this plot: the contributions to the cohesive energy from sp- and d-electrons separate out simply as the areas under the curves from equilibrium to infinite volume. For further discussions, see Pettifor[22], Gellot *et al.* [23] and Anderson *et al.*[24]

Most important, the *s*-band is free-electron-like and cannot be described in tight-binding. As the crystal is compressed, the *s*-electrons are forced closer to the core where their kinetic energy is raised by orthogonality constraints. The bottom of the *s*-band then increases with decreasing volume and the *s*-pressure is positive. The *d*-pressure is negative; indeed, in a simple, orthogonal tight-binding model, one cannot reproduce a positive band pressure, so that the effect of *s*-electrons is best relegated to the repulsive pair term. A second reason to omit the *s*-band is that one cannot build a free-electron-like *s*-band out of tight-binding *s*-functions. One would need to include *p*-orbitals as well, which would make the basis too large for practical purposes.

We do, however, expect to reproduce other equilibrium properties—for example elastic constants and heats of formation of alloys—in which the free-atom energies cancel out. The cancellation is a test of the interaction parameters between Mo and Re: we have imagined a hypothetical MoRe alloy in the ordered bcc (CsCl or B2) structure and used full-potential, self consistent LMTO theory to compute its lattice constant, elastic constants, and heat of formation. We have compared these with the predictions of the self-consistent tight-binding model. We have also used the model to calculate the elastic contants of bcc Mo and the axial ratio of hcp Re and compared these with experiment. The results are displayed in Table 2.

Table 2

CALCULATED EQUILIBRIUM PROPERTIES COMPARED WITH EXPERIMENT OR EXACT THEORY (In parentheses)

(The lattice constant *a* is in bohr, *c/a* is the hcp axial ratio, C′ is $(c_{12}-c_{44})/2$ and *K* is the bulk modulus—these are given in GPa; H_f, the heat of formation, is in mRy/atom.)

	a	*c/a*	*C′*	c_{44}	*K*	H_f
Mo	5.95		112	126	299	
			(151)	(109)	(262)	
Re	5.22	1.610				
		(1.614)				
MoRe	5.89		91	143	340	+1.4
	(5.89)		(89)	(217)	(299)	(+8.5)

The agreement is about what one would expect from a tight-binding theory, and quite acceptable. The most obvious disrepancies are in MoRe, where tight-binding underestimates c_{44} and the heat of formation. It is noteworthy that H_f is positive; *i.e.*, the compound does not exist, and this at least is correctly reproduced. We note also that the elastic constants of pure transition metals are also determined by subtle band-structure effects that are not perfectly reproduced by the tight-binding model.

3.3.2 Structural Stability

It is of extreme importance to test the stability of the tight-binding model against the stability of competing structures, both close-packed fcc, hcp, and bcc and also non-close-packed structures such as simple hexagonal (hex) and simple cubic (sc).[5,20] Energy-volume curves for

these structures for the 3*d* transition series are available[5] for comparison. Figure 5 shows the curves calculated using the tight-binding model. Apart from absolute values of the cohesive energies, which are underestimated (as discussed earlier) owing to lack of *sd*-hybridization in the model, the curves agree with first-principles theory very well. In particular, the energy differences between close-packed phases are in excellent agreement with band theory (Figure 2); the comparison is shown in Table 3.

Table 3

ENERGY DIFFERENCES (In mRy/atom) BETWEEN THE CLOSE-PACKED PHASES OF Mo AND Re

(Results from the tight-binding model are compared with first-principles band theory,[19] in parentheses.)

	bcc-fcc	hcp-fcc
Mo	−27.1	+3.0
	(−34.0)	(+2.6)
Re	+28.3	−2.2
	(+26.4)	(−5.9)

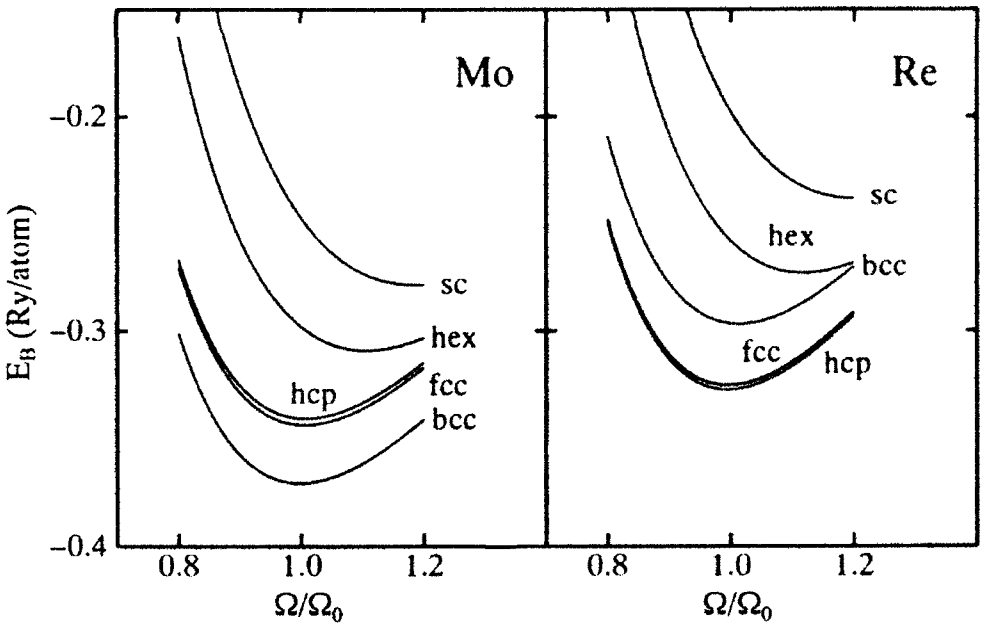

Figure 5. Cohesive energy versus atomic volume Ω. Ω_0 is the equilibrium volume. The curves for Mo and Re are computed using the tight-binding model. Apart from errors in the absolute cohesive energy due to neglect of *sd*-hybridization, they are in very good agreement with what one would expect from a first-principles calculation.[5]

3.3.3 Finite Deformations

As a final test of our model, we calculate the energy as a function of homogeneous lattice deformation. Here, the bcc lattice is given a simple shear on the (112) plane in the $[\bar{1}\,\bar{1}\,1]$ direction until the lattice shears into itself. This is a homogeneous twinning shear. First-principles calculations of the energy versus shear are available for comparison,[25] which is shown in Figure 6.

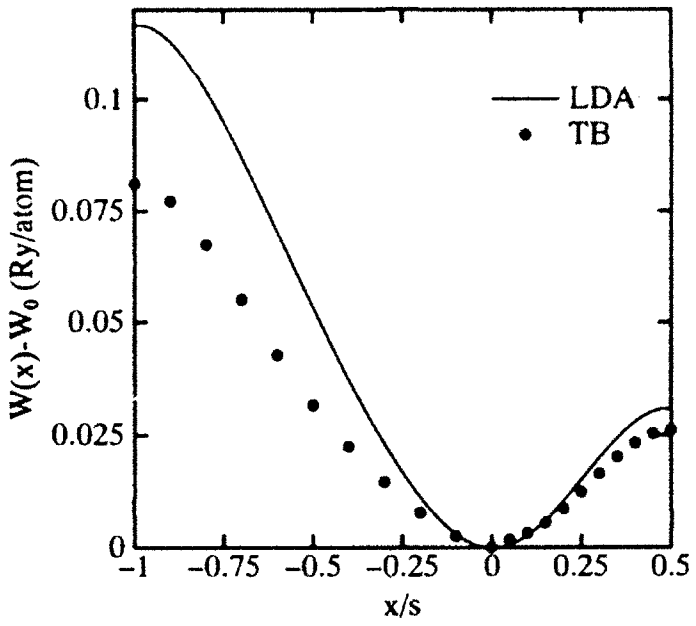

Figure 6. Energy density, W, versus shear x/s. For details see the first-principles calculations of Paxton *et al.*[25]. The agreement between tight-binding and first-principles calculations is excellent in the twinning branch, but rather poorer in the antitwinning branch.

At last, we find quite a large discrepancy between the model and first principles, namely the antitwinning branch of the energy-shear curve in Mo. This is a very large distortion of the lattice away from equilibrium, so the disagreement is not too disturbing. It is well, however, that we have pushed our model far enough to find the point at which it eventually breaks down. Even classical potentials are rarely tested as thoroughly as we have tested the tight-binding model here.

4. RELAXATION AND ATOMIC STRUCTURE

Armed with a quantum mechanical model of the Mo-Re system, we go ahead and compute the atomic structure of our chosen interface. This is done by setting up the unrelaxed interface in [Figure 1(b)], calculating the forces acting between the atoms, and relaxing their positions in a molecular statics algorithm.[12] Even using a simplified quantum mechanical model, this is a very time-consuming business.

We do our calculations in supercells so that we can exploit Bloch's theorem in evaluating the eigenvalue sum in Eq. (4). We do this by a tetrahedron integration over the Brillouin zone, using 72 k-points in the whole zone. The size of the supercells is such that there are eight layers of Re atoms and five layers of Mo before the cell repeats itself along the y-direction (Figure 1). We have done some tests using larger cells and convinced ourselves that the electronic structure is converged at this supercell size. Artificial elastic interactions will remain and persist to very large cell sizes, and we have to live with them.

Because of the complexity of the problem, we are forced to make some further approximations. The separation h between the crystals should, ideally, be relaxed along with the atom positions. Instead, we have determined h for the unrelaxed cell and used that value (4.63 a.u.) as fixed. All relaxations subsequently are at constant volume. We also do the self-consistency procedure separately from the atomic relaxations. That is to say, we first relax the positions and then make the Hamiltonian self-consistent; we have found that further relaxations are not significant. Finally, we calculate the total energy of the supercell using twice the number of k-points.

The range of the Hamiltonian matrix elements $h(r)$ and the pair potential $\varphi(r)$ are usually taken as rather short in tight-binding theory. However, we have chosen not to truncate these until after fifth neighbors in the bcc structure (at $\sqrt{3}a_{\mathrm{bcc}}$) and sixth neighbors in the hcp structure (at $2a_{\mathrm{hcp}}$). This actually improved the band structure somewhat; more important, it devolves from us the responsibility of choosing what are and are not neighbors since, at the cut-off, the matrix elements are insignificantly small. Because we are using a k-space method, the longer range of the interactions does not affect the computing time; in a real-space approach such as the recursion method this would not be economical.

4.1 THE MISFIT DISLOCATION

The relaxed structure of the Mo/Re interface from Figure 1(b) is shown in Figure 7. As expected, to the left and right parts of the interface, the lack of registry (disregistry) between atomic planes across the interface has improved at the expense of the appearance of a dislocation core at the center. In other words, the disregistry, which is evenly distributed across the epitaxial interface, has become localized at the core of a misfit dislocation after atomic relaxation. As far as we know, this is the first quantum mechanical simulation of a dislocation core structure in transition metals. We therefore regard this as a significant step forward. Already we can answer

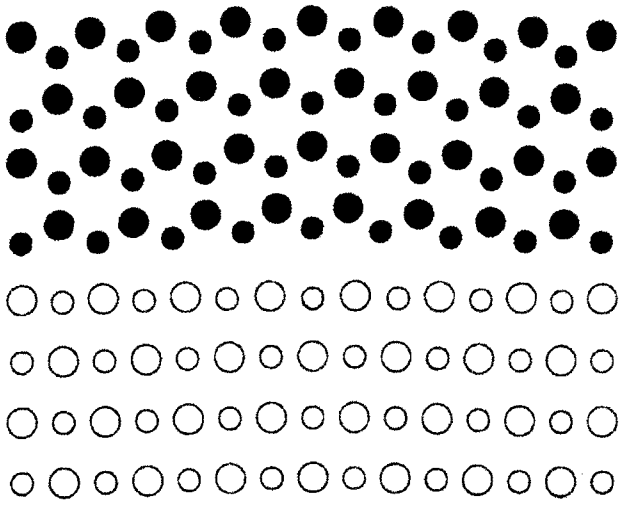

Figure 7. Structure of the relaxed interface. The shaded atom corresponds to that in Figure 1(b) and appears at the core of the misfit dislocation.

our first question of Section 2, as to the width of the core. The width is roughly half the dislocation spacing (there is, of course, an infinite array of dislocations generated by the periodicity along the x-axis).

Let us make a few comments about Figure 7. The relaxation of the Mo layer is confined to some bending of the atomic planes about the z-axis due to long-range elastic effects. These are artifacts of the supercell size mentioned above. The distortions at the core are otherwise confined to the Re layer which moves closer to the Mo in the region of good registry, and away from the Mo at the dislocation core. Therefore, contrary to the Peierls model, there is some bending of the atomic planes.

The position at the interface indicated with a shaded Mo atom in Figure 1(a) turns out to be the center of the core. This is in fact the lowest-energy position for the dislocation, as we shall see below, indicating the position of the Peierls valley. In this alignment, Mo and Re atoms face each other across the interface in the same atomic plane along the z-axis. The interface prefers to remain in registry at positions where Mo and Re atoms face each other in atomic planes at different distances along the z-axis. In other words, referring to Figure 1(b), the interface prefers to maintain the middle region in registry and concentrate the misfit at the edge regions. Put yet another way, referring to Figure 1(a) the body-centering atom, rather than sitting opposite the center of the $(10\bar{1}0)$ face (as shown), prefers to sit along the edge of that face. This is because in the situation shown in Figure 1(a), the shaded Mo atom is closer to its opposite Re atom than the nearest-neighbor distance in the pure metals. The edges of the interface in Figure 1(b) are therefore the high-energy regions and the center is a low-energy region since opposite Mo and Re atoms are in different layers along the z-axis and therefore not too close together. Thus, when the structure relaxes, the high-energy part becomes the core of the dislocation while the the low-energy part remain in registry. Figure 1(b) also represents the lowest-energy configuration for the dislocation. The core lies in a Peierls valley, since if it is to move in the x-direction the disregistry must shift into the region of low energy, which costs energy. Section 4.2 discusses what happens when we try to move the dislocation.

4.2 THE PEIERLS ENERGY

In a series of simulations in molecular statics, we apply successive shear strains to the atomic cell. It is clear from a study of Figure 1(b) that if we displace the (upper) Re block with respect to the (lower) Mo block by a vector of length $b = a_{Mo} - a_{Re} = 0.73$ bohr in the x-direction, then we would recover an identical atomic structure. This is the *translational periodicity* of the interface in the x-direction. In the process, the dislocation will move through a distance b, achieving a plastic strain of the interface. The energy barrier involved in this process is the Peierls energy of the misfit dislocation.

Beginning with the relaxed structure shown in Figure 7, we apply a strain of $0.2b$ by adjusting the boundary conditions of the supercell (see Paxton[26] for details of how this is done). We again relax the atomic positions, make the Hamiltonian self-consistent and, obtain the total energy of the cell for this displacement. Using the new, sheared structure, we apply another strain of $0.1b$ and repeat the procedure. We continue to shear the cell by increments of $0.1b$, relaxing the positions and the Hamiltonian at each step. We obtain a plot of the energy of the cell versus shear, as shown in Figure 8. We show displacements up to only $0.4b$; for larger values we have encountered problems in determining the global minimum from a number of metastable states. By symmetry, however, we know that the curve must be symmetrical about $b/2$ so only that value of the displacement is lacking in the present work.

We can arrive at a very important conclusion from these calculations. As the dislocation moves from one Peierls valley to the next (a distance b away) the energy barrier ΔE is on the order of 3 mRv. The displacement is $b/2$ so that the stress is, very approximately,

$$\tau \approx \frac{2\Delta E}{A_{cell} b}$$

where A_{cell} is the area of the interface in the unit cell. This is about 0.4 GPa which is more than 10 times smaller than the theoretical strength, which must be on the order of 10–20 GPa. Therefore, while the presence of the dislocation clearly reduces the strength of the interface, it does not have as strong an effect as a lattice dislocation, which is expected to reduce the strength of a crystal by several orders of magnitude from the theoretical strength.

Because the tight-binding model can reproduce the theoretical strength of Mo very well compared with a first-principles calculation (see Figure 6) we regard the above result as significant. We repeat our conclusion: the misfit dislocation has the effect of reducing the strength of the interface from the Frenkel theoretical strength, although not by as much as would be expected from a lattice dislocation in a single crystal. Therefore, the presence of misfit dislocations in an otherwise perfect interface is not expected to reduce the strength significantly. On the other hand there is a notable reduction in the theoretical strength compared with a lattice matched interface.

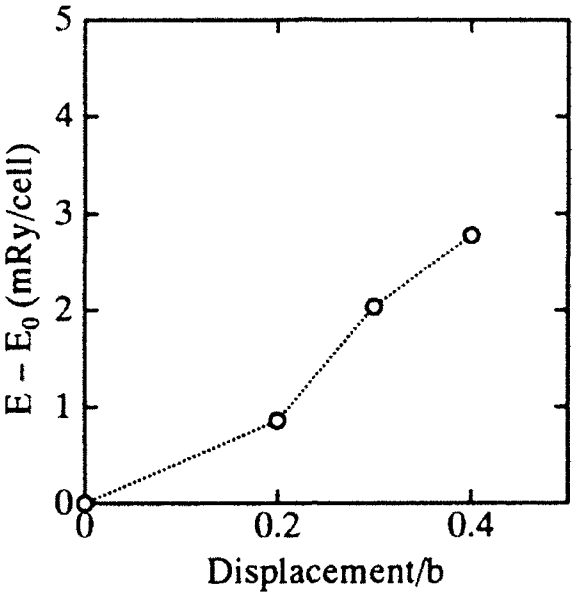

Figure 8. Energy *E* of the interface relative to that of the undisplaced structure E_0 of Figure 7. The displacement is in units of the translational period *b* of the interface.

5. PLAN OF FUTURE WORK

We are confident that the simple tight-binding model is adequate for the study of central transition-metal interfaces. If we want to study transition-metal aluminide alloys, metal-ceramic interfaces, or nonmetal impurities, then we would need to use first-principles density functional theory. As we will see (Section 6) our program of work to develop a first-principles molecular dynamics for all elements in the Periodic Table is sufficiently far ahead for us to regard this extension as becoming feasible in the coming year.

Meanwhile, there is plenty we can learn about dissimilar metal interfaces in general from our tight-binding work. Our plan for future work includes the following:

1. We would like to extend our implementation of the tight-binding method to include molecular dynamics as well as statics. This can be easily done.

2. Now that we know the structure and have an estimate of the strength of the ideal Mo/Re interface, we need to investigate the effect of interdiffusion. This is the realistic case encountered in diffusion bonding, and we want to know how the intermixing of the atoms affects the properties of the interface.

3. We have a way of studying interface dislocations in general, now that we have this nice model of a dislocation which, since it is an interfacial dislocation, has no long-range strain field. We would like to use this model system to study the dislocation point-defect interaction which has not yet been investigated using a serious quantum mechanical model.[26]

6. ADVANCES TOWARDS REAL-SPACE, FIRST-PRINCIPLES MOLECULAR DYNAMICS

As we have mentioned, the tight-binding method is suitable only in certain favorable cases, for example silicon, germanium, and the central transition metals. Eventually we want to be free to study any system, including grain boundary impurities and the metal-ceramic interface. To this end, some of our time under this contract has been spent on continuing development of our new real-space, total-energy method, which is mostly being supported under a separate ONR contract. In this final section, we report on our progress. We begin by reviewing the state of the art in first-principles molecular dynamics.

Extensive research has now established that it is possible to calculate in density functional theory (DFT), and with fairly high accuracy (often comparable to the uncertainties in measurement), a broad range of mechanical and structural properties of most solids. DFT is, in principle, exact: solving it is completely equivalent to solving the many-body Schrödinger equation. The exact functional is unknown, but the important advances in this area have been made using a *local* approximation to the exact functional. The local density approximation (LDA) contains no empirical or adjustable parameters, but makes it possible to obtain an explicit form for the Schrödinger equation that recasts the problem as a set of independent electrons moving in an effective one-electron potential. Its success in predicting—from first principles—mechanical properties such as structural energy differences, defect energies, and shear moduli is remarkable.

Solution of the LDA is technically difficult and computationally demanding. While many problems have been successfully broached within the LDA, in practice limits to computational capacity sharply circumscribe what it can feasibly address. This difficulty, one of practice rather than of principle, is compounded because the computational effort grows rapidly with the complexity of the calculation. The one-electron Hamiltonian $\hat{H}$ is projected onto a basis set, and obtaining the eigenvalues of $\hat{H}$ amounts to the solution of a linear algebraic eigenvalue problem. The size of the basis, and thus of $\hat{H}$, grows in proportion to the number of inequivalent atoms n, making the operations count increase as the cube of n. It is now routine to study systems with fewer than twenty or so inequivalent atoms, but the n^3 barrier rapidly sets in beyond this point. Even this number is quite sufficient to study in detail many materials properties, such as those needed to compute phase diagrams. On the other hand, two important advances are rapidly widening the scope of feasible applications of the LDA. The first has to do with massive parallelization of computer hardware, making the next generation of computers several orders of magnitude more powerful than present-day ones. Fortunately, most electronic structure methods are quite amenable to parallelization; this is especially so with respect to the methods described in the following subsections. The second has to do with significant advances in algorithms used to solve the single-particle Schrödinger equation.

6.1 NEW DEVELOPMENTS IN ELECTRONIC STRUCTURE ALGORITHMS

Because of the immense potential of the LDA to realistically calculate practical material properties, there has been intensive effort to develop algorithms to solve the LDA efficiently. Car and Parrinello[27] precipitated the present efforts by proposing an algorithm to pursue molecular dynamics simulations within the LDA, by introducing a technique that integrates the nuclear and electronic motion into a single step. While their paper attracted a great deal of attention for this reason, actually the most important result of their paper was the introduction of an ingenious scheme to obtain, for a plane-wave (PW) basis, eigenvectors of the Hamiltonian much more efficiently than previously. They exploited the fact that for a PW basis, the kinetic-energy part of the Hamiltonian is diagonal in k-space and the potential is diagonal in real-space. Using a fast Fourier transform to transform a trial eigenvector between the two spaces, they could operate the Hamiltonian on a trial eigenvector far more efficiently than before. Using an iterative scheme to generate the eigenvectors obviates the most costly of the n^3 bottlenecks in solving the band-structure problem. To iterate M trial eigenvectors, χ, in a PW basis of dimension N, the operations count to make $\hat{H}\chi$ is $O(NM \ln N)$. In this procedure, higher lying eigenstates must be orthogonalized to lower ones using a Gram-Schmidt step, which requires $O(M^2N)$ operations. M and N are both proportional to the number of atoms n, so the n^3 bottleneck remains; on a PW basis, however, $N \gg M$ and this method is much more efficient than conventional diagonalization schemes, which require an operations count of order N^3. For moderately sized systems, the Gram-Schmidt step does not seem to dominate the total time. More efficient schemes have since been introduced that allow the iteration of a trial eigenvector to proceed to the eigenstate in fewer steps.[28]

6.2 REAL-SPACE HAMILTONIANS

The Car-Parrinello method (and its modern-day descendants[28]) has been successful for systems of moderate size, but is not generally applicable; in particular, it relies on pseudopotential approximations that make it ill suited to many applications with elements outside of columns III–VII in the Periodic Table. This is a dynamic and rapidly changing subject, to which we cannot do justice here. We will briefly describe new developments we have been pursuing, that show great promise for yet more significant improvements in efficiency. The n^3 barrier is not one of principle, since the electronic Hamiltonian is approximately *local*: well-separated electrons are coupled together only by their (classical) electrostatic interaction and it is unnecessary, in principle, to couple their electronic motion. Thus it must be possible, in principle, to generate solutions to the LDA that increase only linearly with the number of atoms.

By construction, the PW basis is nonlocal, and is not suited to techniques that exploit the local nature of the Hamiltonian. For this, a real-space basis is needed. Real-space basis sets have the following advantages: (1) They are tailored to the potential of the system; thus they are much smaller and more efficient than a PW basis, and the decomposition of eigenstates into local orbitals helps provide physical insight into the problem. (2) Unlike the PW basis, they are generally applicable, and can be equally well adapted to "deep" potentials, such as are encountered in transition metals. (3) A real-space approach is optimally parallelizable. As is well known, the

primary obstacle to massively parallel algorithms arises from delays in *interprocessor communications*. They limit the overall efficiency of most algorithms to a small fraction of a computer's theoretical efficiency. Fortunately, algorithms using a real-space basis can be highly coarse-grained, since a single node can be assigned to one or a small number of atoms, and requires minimal communication with other nodes. (4) Using a real-space basis, it is possible, in principle, to exploit the locality of the Hamiltonian and make the total computation time increase only linearly with the size of the system. Indeed, the recursion method is a strictly real-space technique, for which the computation time increases only as N. With regard to parallelization, the recursion method needs no interprocessor communication at all (with the minor exception of finding the Fermi level of the system as a whole at the end of an iteration).

While the recursion method may be a practicable alternative for large systems, finding yet better ways to diagonalize a real-space Hamiltonian is one key part of our program. For example, it is possible to adapt some of the conjugate-gradient diagonalization techniques[28] in the PW basis to real-space methods, and once again avoid the largest of the n^3 bottlenecks. A real-space Hamiltonian is local and thus sparse for a large system. For a large system, the operation count to make $\hat{H}\chi$ increases with $O(MN)$ in a real-space basis. Both a PW basis and a real-space basis have a Gram-Schmidt orthogonalization step which increases as $O(M^2N)$. However N is an order of magnitude smaller in a real-space basis. Still other approaches can be considered, and study of these forms one key aspect of our research.

6.3 CHOICE OF REAL-SPACE HAMILTONIANS

There are two important drawbacks to a real-space Hamiltonian. The first is that actually constructing such a basis $\{\phi\}$ and calculating matrix elements for it is in general quite difficult, indeed much more complicated than for a PW basis. Any method must carry out the following steps: (1) represent the charge density and solve Poisson's equation for the electrostatic potential; (2) evaluate matrix elements of the Hamiltonian $\langle \phi_1 | \hat{H} | \phi_2 \rangle$, and (3) sum an appropriate linear combination of wave function products $\langle \phi_1 | \phi_2 \rangle$ to generate the output density. All of these steps are simply done using plane waves, but not for general functions Φ. A second major drawback is that, owing to the minimal basis, internuclear forces cannot be reliably calculated from the Hellmann-Feynman theorem, even though knowledge of these forces is essential for molecular dynamics or to relax a large configuration of atoms to their equilibrium positions.

One way to tackle these obstacles is to represent the charge density in PW, but use a local basis for the Hamiltonian. Most real-space methods use this technique, and we employ such a procedure in the present work. For the Hamiltonian, we employ the method of Linear Muffin-Tin Orbitals invented by Andersen.[24] Because its orbitals are tailored to the potential of the solid, the LMTO method employs the most intelligent basis set of all electronic structure methods. Near the nuclei, the wave function is represented numerically and solves the Schrödinger equation essentially exactly. In the interstitial region, the kinetic energy of the envelope functions is customarily set to zero, which is close to the optimal average value for close-packed solids.

An alternative technique, very recently developed by Methfessel and van Schilfgaarde (manuscript in preparation) uses a strictly real-space method, in which both the basis and the density are represented as spatially local, atom-centered functions. This new technique is highly

efficient; to date a molecular program has been completed in which it is possible to calculate the eigenstates of small molecules in a few seconds on a workstation. Here we sketch only the essentials of the method; the paper will be published shortly. In any real-space method, a difficulty immediately arises when attempting to represent the electron density ρ which is calculated from the sum of products of basis functions. There is no convenient analytical representation of Hankel function products that the LMTO method employs (as there is in products of plane waves); which is why most methods resort to plane waves to represent the density. The kernel of the present method centers around an approximate—but analytical—representation of the products of two Hankel functions centered on different sites. The new method approximates such a product as a linear combination of Hankel functions centered on the two separate sites. (This approximation is done once and for all by tabulating a least-squares fit of Hankel function products, so that mapping a product of two functions is essentially a table look-up.) Thus the density ρ can be mapped into a linear combination of atom-centered Hankel functions. In a like manner, matrix elements of the potential $\langle \phi_1 | V | \phi_2 \rangle$ are easily calculated, once again using the mapping $\phi_1 \phi_2 \rightarrow \sum_j c_j \chi_j$.

As with plane-wave representations, the error in the approximation can be made arbitrarily small by increasing the number of functions that approximate a product. The key advantage to this representation is that atom-centered Hankel functions are strictly *local*: they do not extend over all space as do plane waves. Table 4 shows some calculated results for selected small molecules.

Table 4

COMPARISON OF STRUCTURAL PROPERTIES IN SELECTED MOLECULES

(θ are bond angles and ω are vibrational frequencies)

	d (au)		*E (eV)*		*θ (deg)*		*ω (cm^{-1})*	
Molecule	***Calc***	***Expt***	***Calc***	***Expt***	***Calc***	***Expt***	***Calc***	***Expt***
N_2	2.074	2.076	11.34	9.8	—	—	2380	2360
H_2	1.444	1.410	4.91	4.5	—	—	4270	4400
Cu_2	4.124	—	2.97	2.1	—	—	291	330
H_2O	1.833	1.811	11.46	9.5	104.5	104.5	1560; 3700	1600; 3760
H_2S	2.562	2.543	8.95	7.5	91.3	92.3	—	—
H_2Se	2.803	2.779	8.28	—	90.3	91.0	—	—

Also with this method, we have found how to make an exact differention of the LDA Hamiltonian, and thus obtain a proper expression for the forces without resorting to the Hellmann-Feynman (force) theorem. The usual Hellmann-Feynman theorem uses the fact that, at self-consistency, the total energy is stationary to first order with respect to changes in the electron density. Minimal basis sets incur errors, however, because the basis moves with virtual displacements of the nuclei. Our force theorem overcomes this by allowing the basis and charge density to shift rigidly with nuclear displacements. We can do so because they are represented as a superposition of atom-centered functions. Thus we obtain additional terms, and the resulting expression is an essentially exact expression for the force.

To summarize, our new method has several features that can combine the best of many existing electronic structure techniques. It uses an efficient, minimal basis, but at the same time can calculate forces precisely. As a real-space method, it can be exploited to render it highly efficient, and yet accurate.

As yet, we only have a real-space molecule program. The next step is to make a solid-state program based on the same principles. We anticipate that when this is completed in the coming months, we will be able to do molecular dynamics simulations of complex transition metal and metal-ceramic systems which are as rapid as using empirical tight-binding, but are nonetheless completely first-principles in approach.

REFERENCES

1. *Proceedings of the International Symposium on Metal-Ceramic Interfaces, July 1991*, Ed. M. Rühle, *et al.* in *Acta Metall. Mater.*, **40** Suppl. (1992)
2. R.H. Titran, *Advanced Materials and Processes*, **142**, No. 5, 34 (November 1992)
3. B.D. Bryskin, *Advanced Materials and Processes*, **142**, No. 3, 22 (September 1992); J.A. Shields Jr, *op. cit.*, **142**, No. 4, 28 (October 1992)
4. M.W. Finnis and J.E. Sinclair, *Phil. Mag. A*, **50**, 45 (1984)
5. A.T. Paxton, M. Methfessel, and H.M. Polatoglou, *Phys. Rev. B*, **41**, 8127 (1990)
6. M. van Schilfgaarde, AT. Paxton, A. Pasturel, and M. Methfessel, *Proc. MRS Symp.* Vol 186; *Alloy Phase Stability and Design*, Eds. G.M. Stocks *et al.*, 107 (1991)
7. A.P. Sutton, M.W. Finnis, D.G. Pettifor, and Y. Ohta, *J. Phys.* C, **21**, 35 (1988)
8. A.T. Paxton, A.P. Sutton, and C.M.M. Nex, *J. Phys. C*, **20**, L263 (1987)
9. J.A. Majewski and P. Vogl, *The Structures of Binary Compounds*, Eds. F.R. de Boer and D.G. Pettifor, Amsterdam, Elsevier Science Publishers, p. 287 (1989)
10. W. A. Harrison, *Phys. Rev. B*, **31**, 21 (1985)
11. M.O. Robbins and L.M. Falicov, *Phys. Rev. B*, **29**, 1333 (1984)
12. A.T. Paxton and A.P. Sutton, *Acta Metall.*, **37**, 1693 (1989)
13. D.J. Chadi, *Phys. Rev. B*, **41**, 1062 (1978)
14. M. Kohyama *et al.*, *J. Phys. C*, **21**, 3205 (1988)
15. J. Friedel, *Trans. AIME*, **230**, 616 (1964)
16. W.M.C. Foulkes and R. Haydock, *Phys. Rev. B*, **39**, 12520 (1989)
17. V. Heine, *Solid State Phys.*, **35**, 1 (1980)
18. D. Spanjaard and M.C. Desjonquères, *Phys. Rev. B*, **30**, 4822 (1984)
19. H.L. Skriver, *Phys. Rev. B*, **31**, 1909 (1985)
20. A.T. Paxton, *Atomistic Simulation of Materials: Beyond Pair Potentials*, Eds. V. Vitek and D.J. Srolovitz, New York, Plenum, p. 327 (1989)
21. B. Legrand *et al.*, *J. Phys. C*, **19**, 4463 (1984)
22. D.G. Pettifor, *J. Phys. F*, **7**, 613 (1977)

23. C.D. Gellat Jr., H. Ehrenreich, and R.E. Watson, *Phys. Rev. B*, **15**, 1613 (1977)

24. O.K. Andersen, O. Jepsen and D. Glotzel, *Highlights of Condensed Matter Theory*, Eds. F. Bassani *et al.*, Amsterdam, North Holland, p. 59 (1985)

25. A.T. Paxton, P. Gumbsch, and M. Methfessel, *Phil Mag. Letters*, **63**, 267 (1991)

26. A.T. Paxton, *Electron Theory in Alloy Design*, Eds. D.G. Pettifor and A.H. Cottrell, London, Inst. Materials, p. 158 (1992)

27. R. Car and M. Parrinello, *Phys. Rev. Lett.* **55**, 2471 (1985)

28. M. P. Teter, M.C. Payne, and D.C. Allan, *Phys. Rev. B*, **40**, 12255 (1989)